Electroweak measurements in CMS

Luca Della Penna
INFN and University of Perugia, Italy
on behalf of the CMS Collaboration

XXXI Cracow EPIPHANY Conference
13-17 January 2025

Contents

Contents:

- Some of the most recent public results from the CMS collaboration, published or submitted during 2024, including the first Run-3 analysis (data taken at 13.6 TeV, starting in 2022)

EW measurements covers various aspects:

- SM parameters extraction (such as boson masses, BRs, EW angle etc.)
- cross-sections of single and multibosons production
- Searches for BSM effects, e.g. through VBS

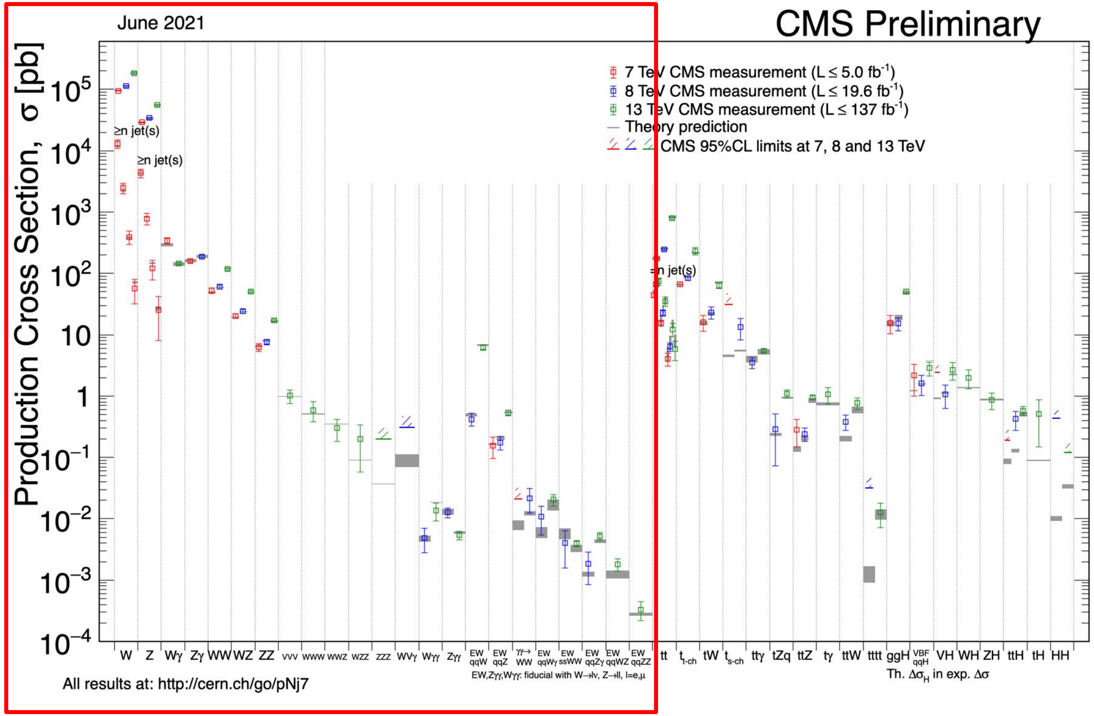

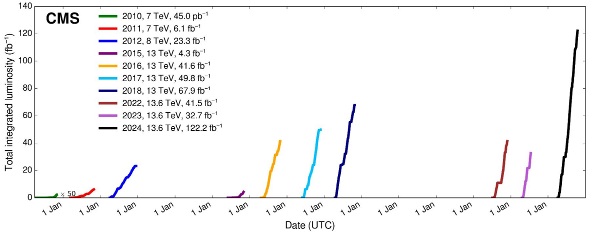

The Backward-Forward asymmetry is used to extract $\sin^2\theta_{EW}$ due to vector and axial current interference. $Z \rightarrow l^+l^-$

$$\frac{1}{\sigma}\frac{d\sigma}{d\cos\theta d\Phi} \sim 1 + \cos^2\theta + \sum_{i=0}^{7} A_i f_i(\theta, \Phi)$$

- Collins-Soper reference frame is used, and the direct extraction from angle between the negative lepton and the incoming quark $\cos\theta_{sc}$ is employed as a cross-check
- Four exclusive categories based on subdetectors information: ECAL (g), HCAL (h) for electrons

	$\lvert\eta\rvert$		$p_{T,min}^{leading}$	$p_{T,min}^{trailing}$
$\mu\mu$	0.00–2.40		20 GeV	10 GeV
ee	0.00–2.50		25 GeV	15 GeV
	$\lvert\eta_e\rvert$	$\lvert\eta_{g,h}\rvert$	$p_{T,min}^{e}$	$p_{T,min}^{g,h}$
eg	0.00–2.50	2.50–2.87	30 GeV	20 GeV
eh	1.57–2.50	3.14–4.36	30 GeV	20 GeV

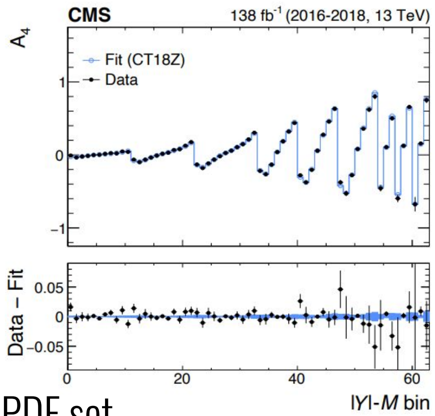

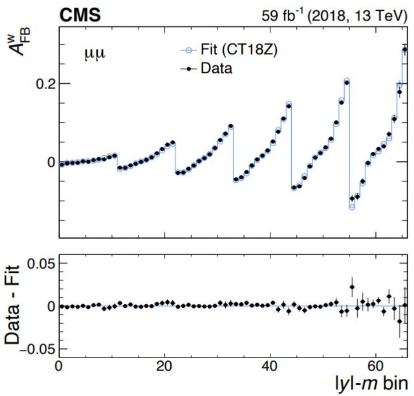

CT18Z PDF set

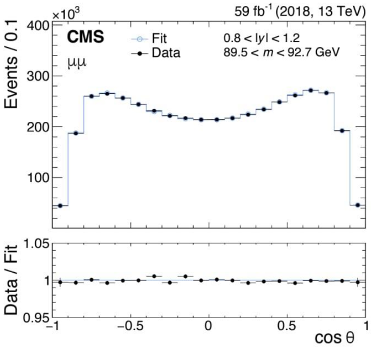

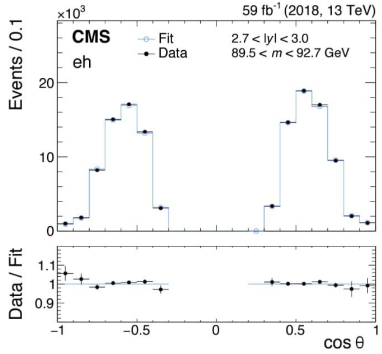

EW angle using the dilepton final state from Z decay is extracted with:
1 - unfolded A_4(|y|, m)
2- weighted A_{FB}(|y|, m) (same method used in Run2 data sample)

SMP-22-010
Submitted to Phys.Lett.B

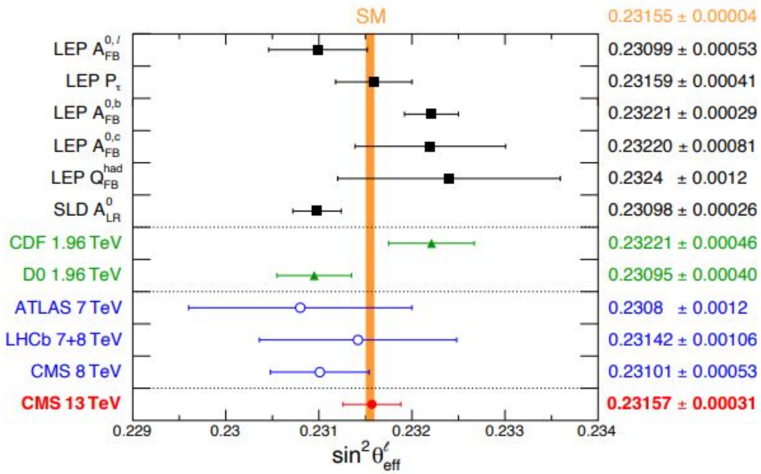

$$Z \rightarrow l^+l^-$$

$$sin^2\theta_{EW} = 0.23157 \pm 0.00031$$

- The most precise measurement at hadron collider
- Comparable to the most precise measurement from LEP and SLD e^+e^- colliders, which differs by 3.2 s.d.
- The uncertainty is dominated by PDFs

Results using the three different methods for all categories and the data-taking periods

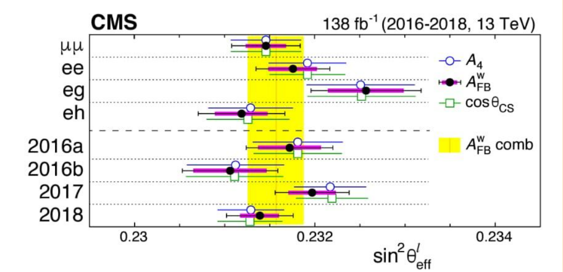

Comparison between alternative choices of PDF sets w.r.t the CT18Z set

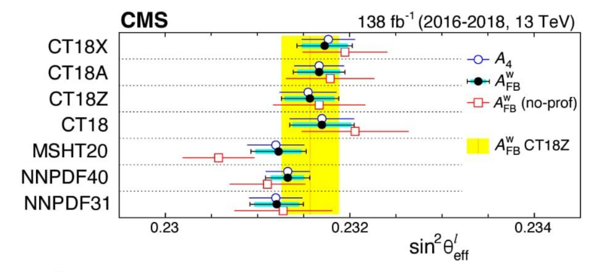

[SMP-22-010](SMP-22-010)
Submitted to Phys.Lett.B

W Branching Fraction

Run2
13 TeV
138 fb^{-1}

Test of CKM matrix unitarity $\sum_i |V_{ci}|^2 = 1$

$$t \to W^+ b \to c\bar{q}b$$

Extraction through semileptonic decay of t-tbar
- Need to tag jets from charm hadronization (moun-tagging technique)

Tagging charm jets

In around 9% of the cases, a muon is produced in charmed-hadron decays

- isolation of the muon within R=0.4 jets: $I_\mu > 2.5$ GeV
- cuts on the p_T^μ fraction of the muon inside the jet to reduce contamination from prompt muons: $p_T^\mu/p_T^{jet} < 0.5$
- calibrated on b-jets
- OS w.r.t the lepton from the other W boson

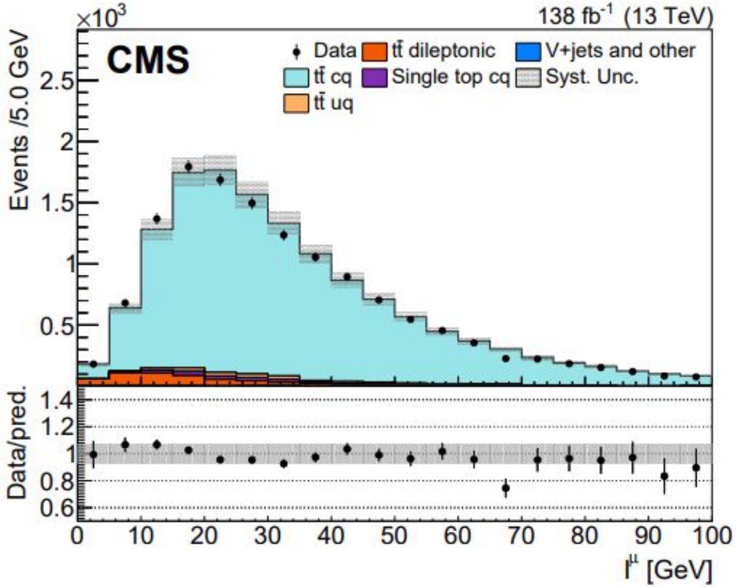

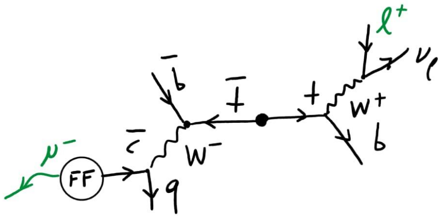

$$R_c^W = \frac{\mathcal{B}(W \to cq)}{\mathcal{B}(W \to uq) + \mathcal{B}(W \to cq)} = \frac{|V_{cd}|^2 + |V_{cs}|^2 + |V_{cb}|^2}{|V_{ud}|^2 + |V_{us}|^2 + |V_{ub}|^2 + |V_{cd}|^2 + |V_{cs}|^2 + |V_{cb}|^2} \overset{\text{CKM unitarity}}{=} 0.5$$

SMP-24-009
Submitted to Phys.Lett.B

W Branching Fraction

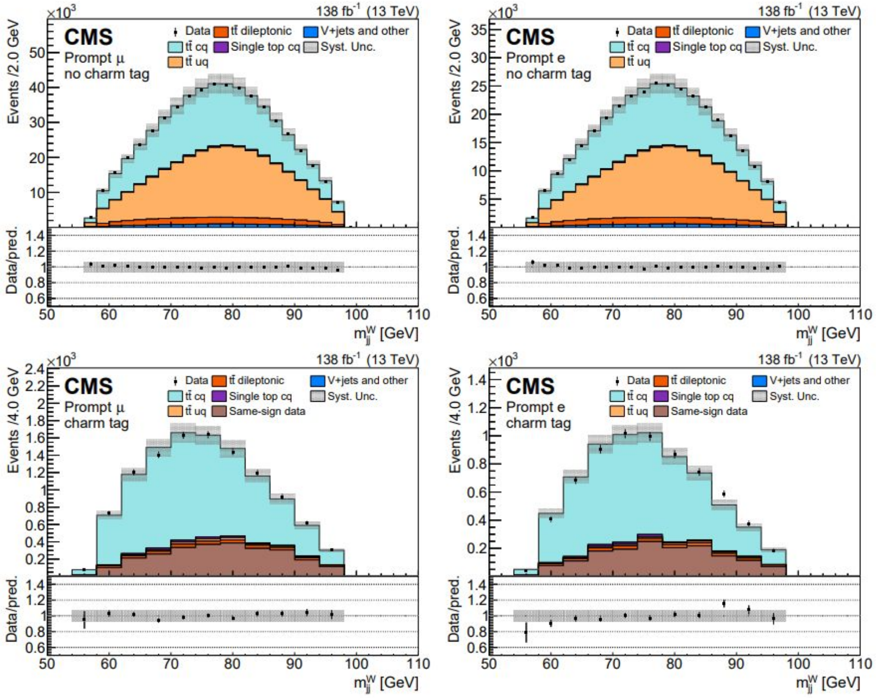

Four categories based on the leptons from a W boson and the tagged charm:

- isolated muon, no charm tag
- isolated electron, no charm tag

- isolated muon, charm tag
- isolated electron, charm tag

Process	Prompt μ no charm tag	Prompt e no charm tag	Prompt μ charm tag	Prompt e charm tag
$t\bar{t}$, W $\to$ cq	245 816 (7%)	151 570 (7%)	8172 (9%)	4993 (9%)
$t\bar{t}$, W $\to$ uq	257 789 (7%)	159 146 (7%)	150 (9%)	84 (9%)
Dileptonic $t\bar{t}$	31 343 (7%)	19 219 (7%)	299 (8%)	188 (8%)
Single top, W $\to$ cq	5060 (7%)	3085 (7%)	133 (10%)	93 (10%)
Single top, W $\to$ uq	4772 (7%)	2948 (7%)	2 (50%)	2 (50%)
Single top, no W $\to q\bar{q}'$	3620 (13%)	1884 (13%)	15 (20%)	9 (50%)
V + jets	5005 (12%)	3687 (12%)	43 (30%)	9 (50%)
Diboson	299 (12%)	142 (12%)	1 (50%)	1 (50%)
Total predictions OS − SS			8815 (9%)	5379 (9%)
Data SS			2551 (2%)	1546 (2%)
Total predictions	553 705 (7%)	341 681 (7%)	11 366 (7%)	6925 (7%)
Data OS	553 378	341 232	11 167	6806

$$R_c^W = \frac{\mathcal{B}(W \to cq)}{\mathcal{B}(W \to uq) + \mathcal{B}(W \to cq)} = \frac{|V_{cd}|^2 + |V_{cs}|^2 + |V_{cb}|^2}{|V_{ud}|^2 + |V_{us}|^2 + |V_{ub}|^2 + |V_{cd}|^2 + |V_{cs}|^2 + |V_{cb}|^2}$$

SMP-24-009
Submitted to Phys.Lett.B

W Branching Fraction

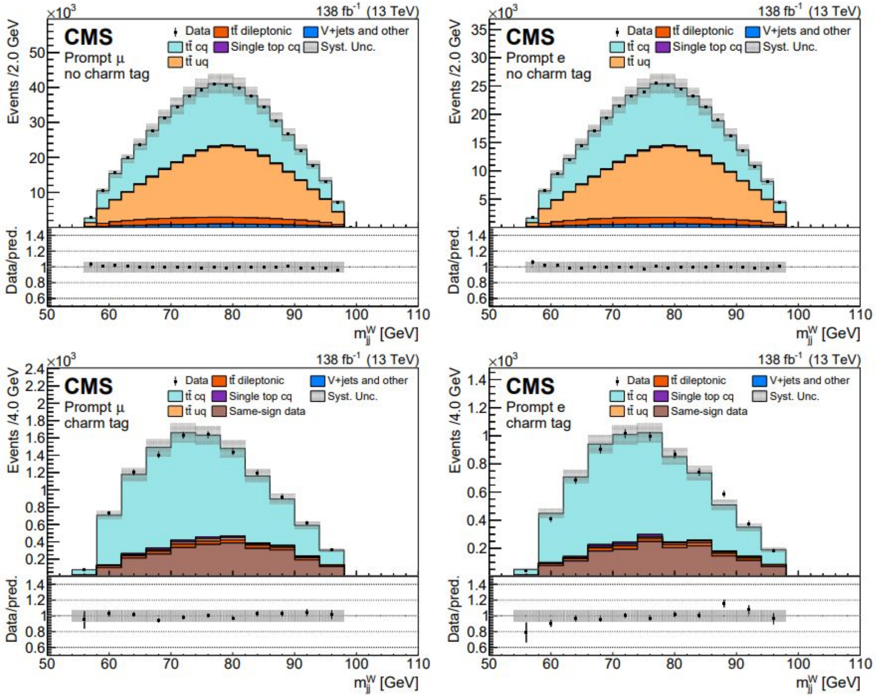

Four categories based on the leptons from a W boson and the tagged charm:

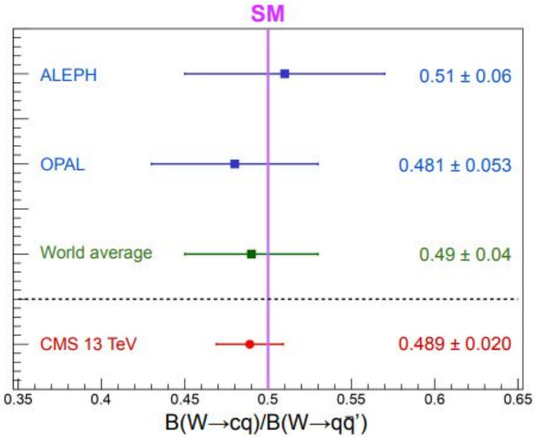

The most precise measurement to date of the W boson hadronic decay branching fraction ratio.

$$R_c^W = 0.489 \pm 0.020$$

$$R_c^W = \frac{\mathcal{B}(W \to cq)}{\mathcal{B}(W \to uq) + \mathcal{B}(W \to cq)} = \frac{|V_{cd}|}{|V_{ud}|^2 + |V_{us}|^2 + |V_{ub}|^2 + |V_{cd}|^2 + |V_{cs}|^2 + |V_{cb}|^2}$$

SMP-24-009
Submitted to Phys.Lett.B

WZ Production Cross Section

Run3
13.6 TeV
34.7 fb^{-1}

CMS collaboration has measured the inclusive cross section of WZ production at all the energies reached by the LHC (5,7,8 and 13 TeV).

- Both inclusive and exclusive WZ cross sections have been measured in leptonic final states (3 isolated light leptons + 1 neutrino)
- requiring exactly three isolated leptons with at least two OSSF leptons to be consistent with Z mass

$$|m(l_Z^{(1)}, l_Z^{(2)}) - m_Z| < 15 GeV$$

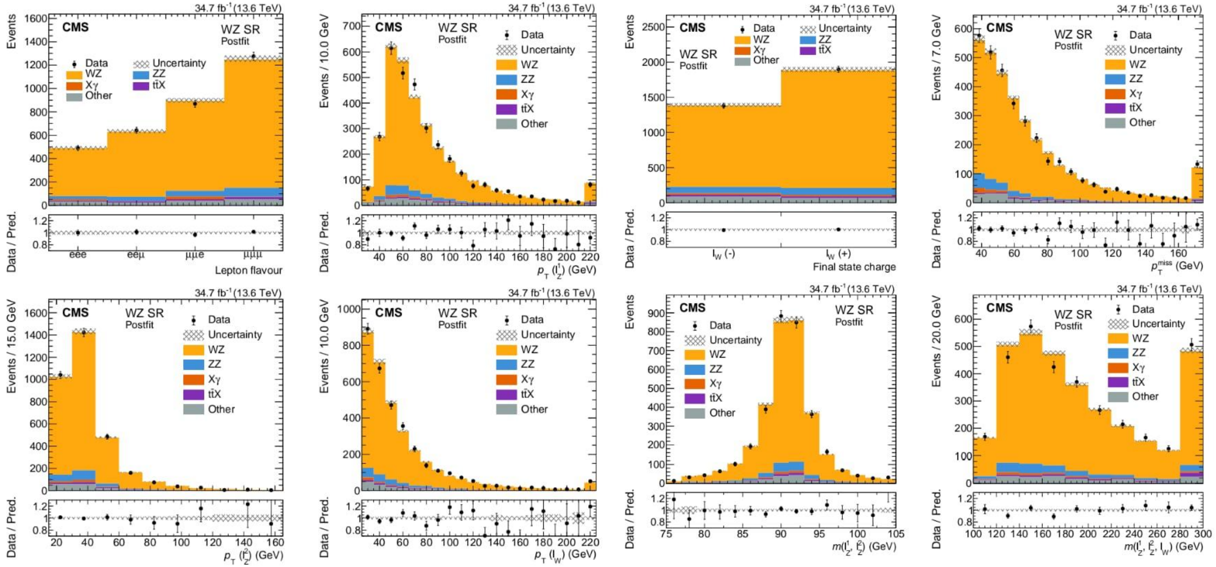

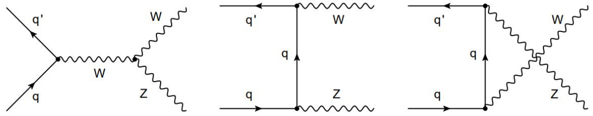

LO Feynman diagrams

Region	N_ℓ	$p_T\{\ell_Z^1, \ell_Z^2, \ell_W(\ell_3), (\ell_4)\}$ (GeV)	N_{OSSF}	$\lvert m(\ell_Z^1, \ell_Z^2) - m_Z \rvert$ (GeV)	p_T^{miss} (GeV)	$N_{b\ tag}$	$\min(m(\ell, \ell'))$ (GeV)	$m(\ell_Z^1, \ell_Z^2, \ell_W(\ell_3))$ (GeV)
SR	=3	>{25, 15, 25}	≥1	<15	>35	=0	>4	>100
ZZ CR	=4	>{25, 15, 25, 15}	≥1	<15	—	=0	>4	>100
$t\bar{t}Z$ CR	=3	>{25, 15, 25}	≥1	<15	>35	>0	>4	>100
$X\gamma$ CR	=3	>{25, 15, 25}	≥1	—	≤35	=0	>4	<100

Run3 Analysis

SMP-24-005
Submitted to JHEP

WZ Production Cross Section

Run3
13.6 TeV
34.7 fb^{-1}

CMS collaboration has measured the inclusive cross section of WZ production at all the energies reached by the LHC (5,7,8 and 13 TeV).

- Both inclusive and exclusive WZ cross sections have been measured in leptonic final states (3 isolated light leptons + 1 neutrino)
- requiring exactly three isolated leptons with at least two OSSF leptons to be consistent with Z mass

$$|m(l_Z^{(1)}, l_Z^{(2)}) - m_Z| < 15 GeV$$

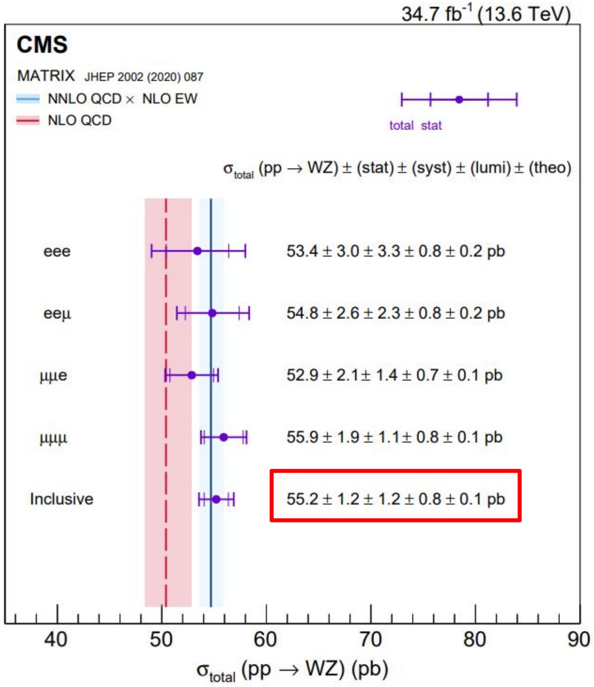

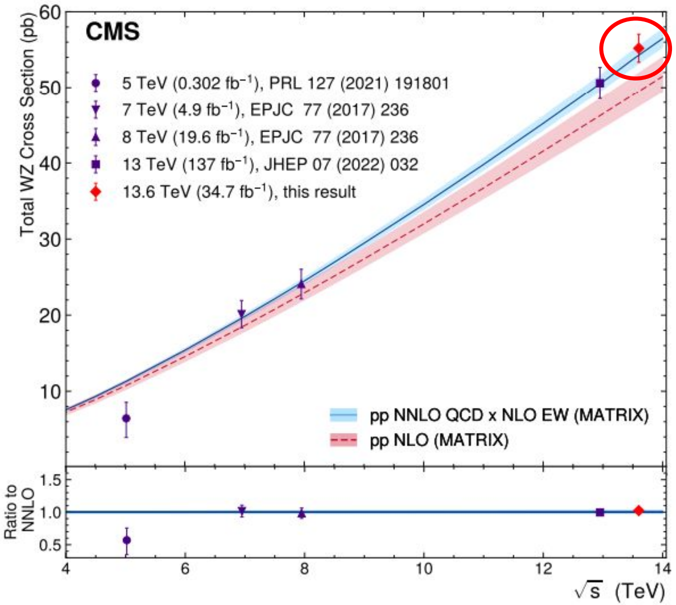

good agreement with SM predictions with MATRIX, NNLO QCD x NLO EW

Run3 Analysis

SMP-24-005
Submitted to JHEP

W^+W^- Production Cross Section

CMS collaboration has measured the inclusive cross section of OS WW production at different energies reached by LHC (7,8 and 13 TeV).

- Both the inclusive total WW cross section and the differential in jet multiplicity have been measured
- requiring two oppositely charged, high-p_T, isolated leptons, including those from leptonic tau decays

$$W^+W^- \to e^{\pm}\nu\mu^{\pm}\nu$$

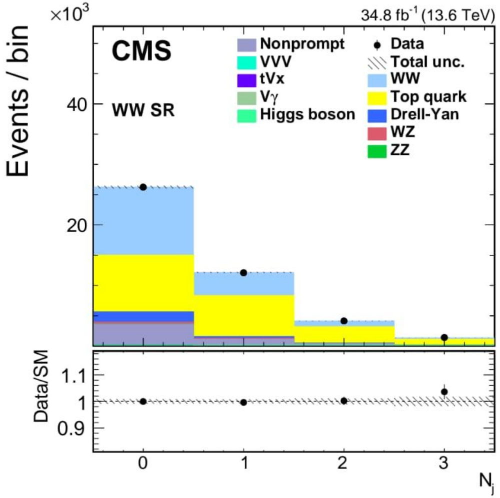

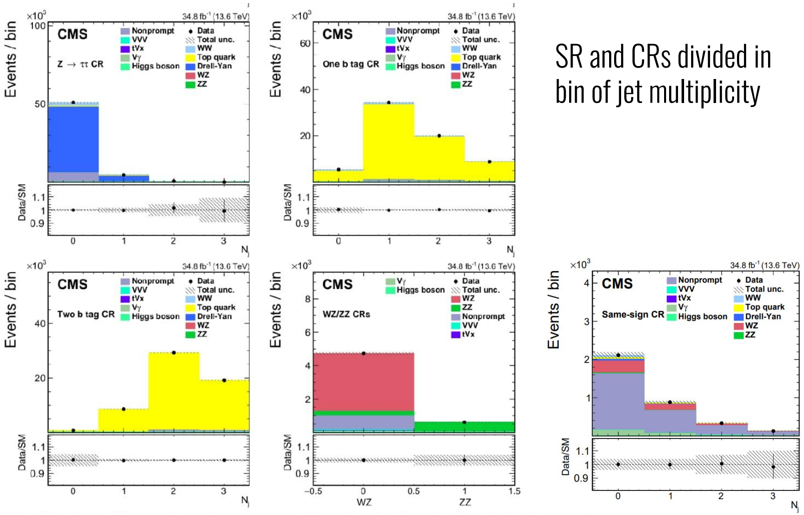

SR and CRs divided in bin of jet multiplicity

Quantity	WW	One/two b tags	$Z \to \tau\tau$	Same-sign
Number of tight leptons		Strictly 2		
Additional loose leptons		0		
Lepton charges		Opposite		Same
$p_T^{\ell\,max}$		>25 GeV		
$p_T^{\ell\,min}$		>20 GeV		
$m_{\ell\ell}$	>85 GeV	>85 GeV	<85 GeV	>85 GeV
$p_T^{\ell\ell}$	—	—	<30 GeV	—
Number of b-tagged jets	0	1/2	0	0
N_j		$0/1/2/\geq 3$		

Variable	WZ	ZZ
Number of tight leptons	Strictly 3	Strictly 4
Additional loose leptons	0	
Lepton p_T	>25/10/20 GeV	>25/20/10/10 GeV (p_T ordered)
$\lvert m_{\ell\ell} - m_Z \rvert$	<15 GeV	<15 GeV (both pairs)
$m_{3\ell}$	>100 GeV	—
$m_{4\ell}$	—	>150 GeV
p_T^{miss}	>30 GeV	—
Number of b-tagged jets	0	

Run3 Analysis

SMP-24-001
Accepted by Phys.Lett.B

W^+W^- Production Cross Section

CMS collaboration has measured the inclusive cross section of OS WW production at different energies reached by LHC (7,8 and 13 TeV).

- Both the inclusive total WW cross section and the differential in jet multiplicity have been measured
- requiring two oppositely charged, high-p_T, isolated leptons, including those from leptonic tau decays

$$W^+W^- \to e^\pm \nu \mu^\pm \nu$$

The cross section is extracted using binned maximum likelihood from observed yields in N_j jet multiplicity bins

$$\sigma(WW) = 125.7 \pm 5.6 \text{ pb}$$

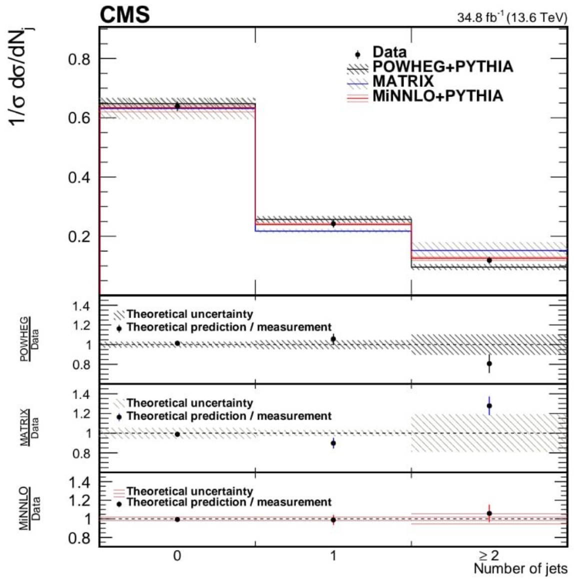

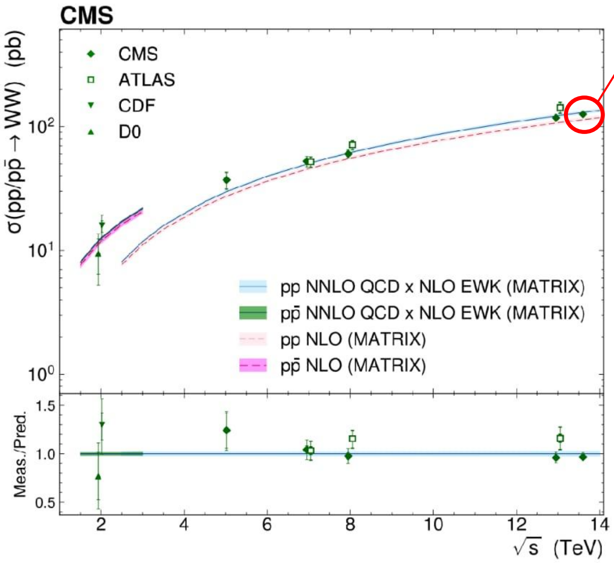

- The inclusive WW cross section is in good agreement with SM predictions using MATRIX, NNLO QCD × NLO EW.
- The differential cross section as a function of the number of jets is in agreement with predictions from POWHEG+PYTHIA, MATRIX NNLO QCD × NLO EW, and MiNNLO+PYTHIA.

Run3 Analysis

SMP-24-001
Accepted by Phys.Lett.B

Vector Boson Scattering

- Vector Boson Scattering is the SM process with the lowest cross section measured by the CMS collaboration to date (can be a < 1 fb).
- Many results in the last few years, since the first observation in 2017
- It is not only a test of SM predictions but also a way for beyond-SM effects

It is sensitive to modification of triple and quartic gauge couplings, which are included in the lagrangian in EFT theories (Wilson coefficients)

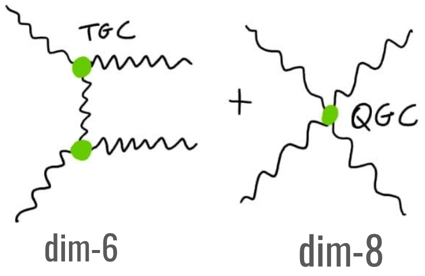

$$\mathcal{L}_{\mathrm{eff}} = \mathcal{L}_{\mathrm{SM}} + \sum_{D_\alpha > 4} \sum_{\alpha} \frac{c_\alpha^{(D_\alpha)}}{\Lambda_{\mathrm{BSM}}^{D_\alpha - 4}} \mathcal{O}_\alpha^{(D)}$$

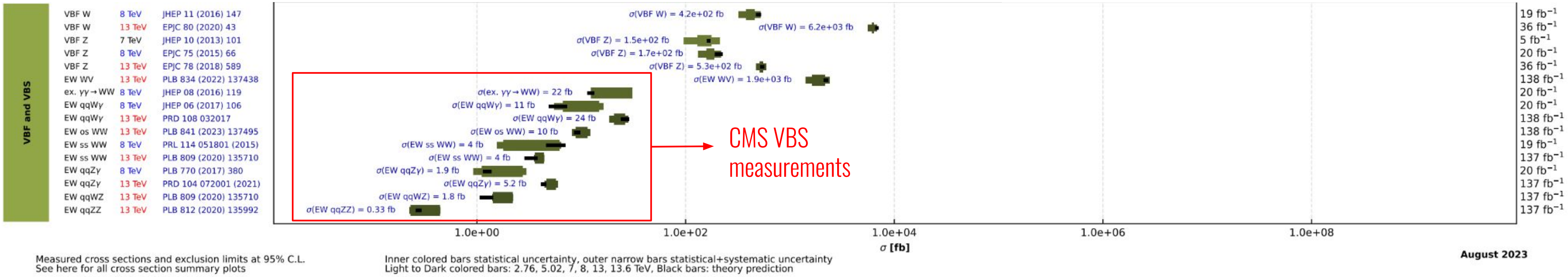

ssWW Vector Boson Scattering

$$W^{\pm}W^{\pm} \rightarrow l^{\pm}\nu_l\tau_h^{\pm}\nu_\tau$$

Indirect search of BSM effects constraints dim-6 and dim-8 EFT operator
The amplitude changes with the new terms:

$$|\mathcal{A}_{\mathrm{BSM}}|^2 = \sum_i^{D_i>4}\left[\frac{c_i^{(D_i)}}{\Lambda_{\mathrm{BSM}}^{D_i-4}}2\,\mathrm{Re}|\mathcal{A}^*_{\mathrm{SM}}\mathcal{A}_{\mathcal{O}_i^{(D_i)}}| + \frac{c_i^{(D_i)^2}}{\Lambda_{\mathrm{BSM}}^{2(D_i-4)}}|\mathcal{A}_{\mathcal{O}_i^{(D_i)}}|^2\right]$$
$$+ \sum_{j\neq k}^{D_j,D_k>4}\frac{c_j^{(D_j)}c_k^{(D_k)}}{\Lambda_{\mathrm{BSM}}^{D_j+D_k-8}}\mathrm{Re}|\mathcal{A}^*_{\mathcal{O}_j^{(D_j)}}\mathcal{A}_{\mathcal{O}_k^{(D_k)}}|, <$$

- at least two jets with large pseudorapidity separation
- exactly one light lepton and one tau lepton with same-sign

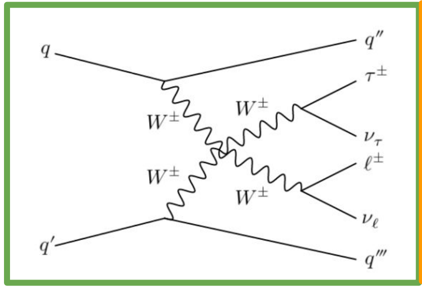

EW ssWW VBS

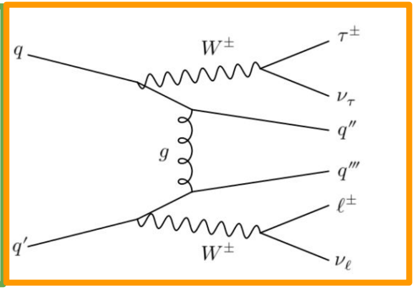

QCD ssWW

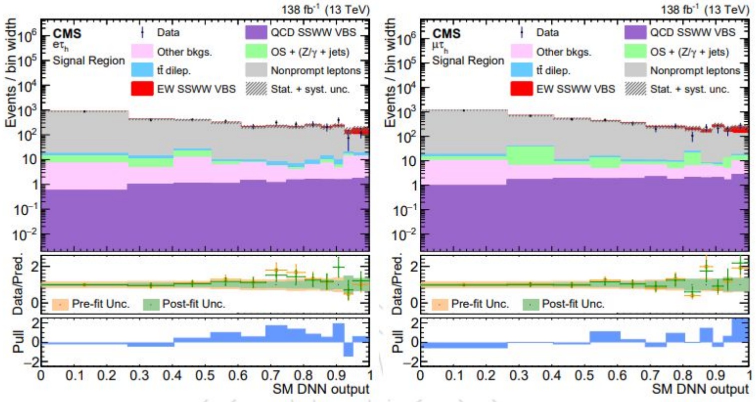

SR DNN outputs

Region	$1\,\mathrm{T}\,\ell, 1\,\mathrm{T}\,\tau_h$, any $\mathrm{L}\,\ell/\tau_h$	>= 2 jets with $\lvert\Delta\eta\rvert > 2.5$	SS ℓ, τ_h	p_T^{miss} >50 GeV	Additional requirements
SR	✓	✓	✓	✓	m_{jj} >500 GeV
Nonprompt CR	✓	✓	✓	×	
tt̄ CR	✓	✓	×	✓	b-tagged jet ("medium")
OS CR	✓	✓	×	✓	b-tagged jet veto ("loose")

- signal strength for EW ssWW VBS is found to be 1.44 times w.r.t SM with 2.6σ significance
- first VBS analysis with a tau lepton in the final state

SMP-22-008
Submitted to JHEP

ssWW Vector Boson Scattering

Run2
13 TeV
138 fb^{-1}

Indirect search of BSM effects constraints dim-6 and dim-8 EFT operator
Extraction of dim-6 and dim-8 coefficients from scan likelihood fit

- one active operator at a time (dim-6 or dim-8) putting to zero all the others contributions
- 2D likelihood scan with 2 active dimension six operators
- 2D likelihood scan with one dim-6 + one dim-8 operator

$$N^i_{\mathrm{exp}} = N_{\mathrm{SM}} + \frac{c_i}{\Lambda^2} N^i_{\mathrm{Lin}} + \frac{c_i^2}{\Lambda^4} N^i_{\mathrm{Quad}}$$

$$N^\alpha_{\mathrm{exp}} = N_{\mathrm{SM}} + \frac{f_\alpha}{\Lambda^4} N^\alpha_{\mathrm{Lin}} + \frac{f_\alpha^2}{\Lambda^8} N^\alpha_{\mathrm{Quad}}$$

Wilson coefficient		68% CL interval(s) Observed	68% CL interval(s) Expected	95% CL interval Observed	95% CL interval Expected
dim-6	$c_{ll}^{(1)}/\Lambda^2$	$[-11.6, 0.045]$	$[-12.9, -8.03] \cup [-2.95, 1.91]$	$[-13.5, 2.11]$	$[-14.6, 3.53]$
	$c_{qq}^{(1)}/\Lambda^2$	$[-0.341, 0.416]$	$[-0.501, 0.576]$	$[-0.605, 0.681]$	$[-0.742, 0.818]$
	c_W/Λ^2	$[-0.513, 0.481]$	$[-0.681, 0.669]$	$[-0.842, 0.818]$	$[-0.987, 0.974]$
	c_{HW}/Λ^2	$[-5.48, 4.31]$	$[-7.00, 6.09]$	$[-8.68, 7.60]$	$[-9.99, 9.05]$
	c_{HWB}/Λ^2	$[-30.7, 89.2]$	$[-41.7, 69.6]$	$[-49.7, 110]$	$[-66.6, 96.4]$
	$c_{H\Box}/\Lambda^2$	$[-12.0, 14.0]$	$[-16.6, 18.1]$	$[-20.9, 22.7]$	$[-24.7, 26.3]$
	c_{HD}/Λ^2	$[-15.3, 31.5]$	$[-24.6, 34.7]$	$[-31.4, 45.5]$	$[-38.2, 48.8]$
	$c_{Hl}^{(1)}/\Lambda^2$	$[-38.2, 39.5]$	$[-28.8, 29.9]$	$[-69.3, 68.3]$	$[-49.4, 49.7]$
	$c_{Hl}^{(3)}/\Lambda^2$	$[-0.045, 8.58]$	$[-1.43, 2.23] \cup [5.88, 9.54]$	$[-1.59, 9.94]$	$[-2.64, 10.8]$
	$c_{Hq}^{(1)}/\Lambda^2$	$[-3.27, 3.44]$	$[-4.53, 4.42]$	$[-5.55, 5.60]$	$[-6.56, 6.44]$
	$c_{Hq}^{(3)}/\Lambda^2$	$[-1.88, 0.705]$	$[-2.39, 1.37]$	$[-2.82, 1.61]$	$[-3.24, 2.16]$
dim-8	f_{T0}/Λ^4	$[-0.774, 0.842]$	$[-1.02, 1.08]$	$[-1.32, 1.38]$	$[-1.52, 1.58]$
	f_{T1}/Λ^4	$[-0.319, 0.381]$	$[-0.426, 0.480]$	$[-0.552, 0.613]$	$[-0.640, 0.695]$
	f_{T2}/Λ^4	$[-0.851, 1.12]$	$[-1.15, 1.37]$	$[-1.51, 1.76]$	$[-1.75, 1.98]$
	f_{M0}/Λ^4	$[-8.07, 7.70]$	$[-9.89, 9.74]$	$[-13.1, 12.8]$	$[-14.6, 14.5]$
	f_{M1}/Λ^4	$[-9.54, 11.15]$	$[-12.5, 13.3]$	$[-16.4, 17.7]$	$[-18.7, 19.6]$
	f_{M7}/Λ^4	$[-17.6, 15.3]$	$[-20.3, 19.2]$	$[-27.6, 25.8]$	$[-29.9, 28.8]$
	f_{S0}/Λ^4	$[-9.60, 9.82]$	$[-11.6, 12.0]$	$[-15.9, 16.1]$	$[-17.4, 17.9]$
	f_{S1}/Λ^4	$[-40.9, 41.3]$	$[-37.4, 38.8]$	$[-60.9, 61.8]$	$[-57.2, 58.6]$
	f_{S2}/Λ^4	$[-40.9, 41.3]$	$[-37.4, 38.8]$	$[-60.9, 61.8]$	$[-57.2, 58.6]$

SMP-22-008
Submitted to JHEP

ssWW Vector Boson Scattering

Indirect search of BSM effects constraints dim-6 and dim-8 EFT operators
Extraction of dim-6 and dim-8 coefficients from scan likelihood fit

- one at a time (dim-6 or dim-8) putting to zero all the others
- 2D likelihood scan with 2 active dimension six operators
- 2D likelihood scan with one dim-6 + one dim-8 operator

$$N_{\text{exp}}^{i,j} = N_{\text{SM}} + \sum_{k=i,j}\left(\frac{c_k}{\Lambda^2}N_{\text{Lin}}^{k} + \frac{c_k^2}{\Lambda^4}N_{\text{Quad}}^{k}\right) + \frac{c_i c_j}{\Lambda^4}N_{\text{Cross}}^{ij}$$

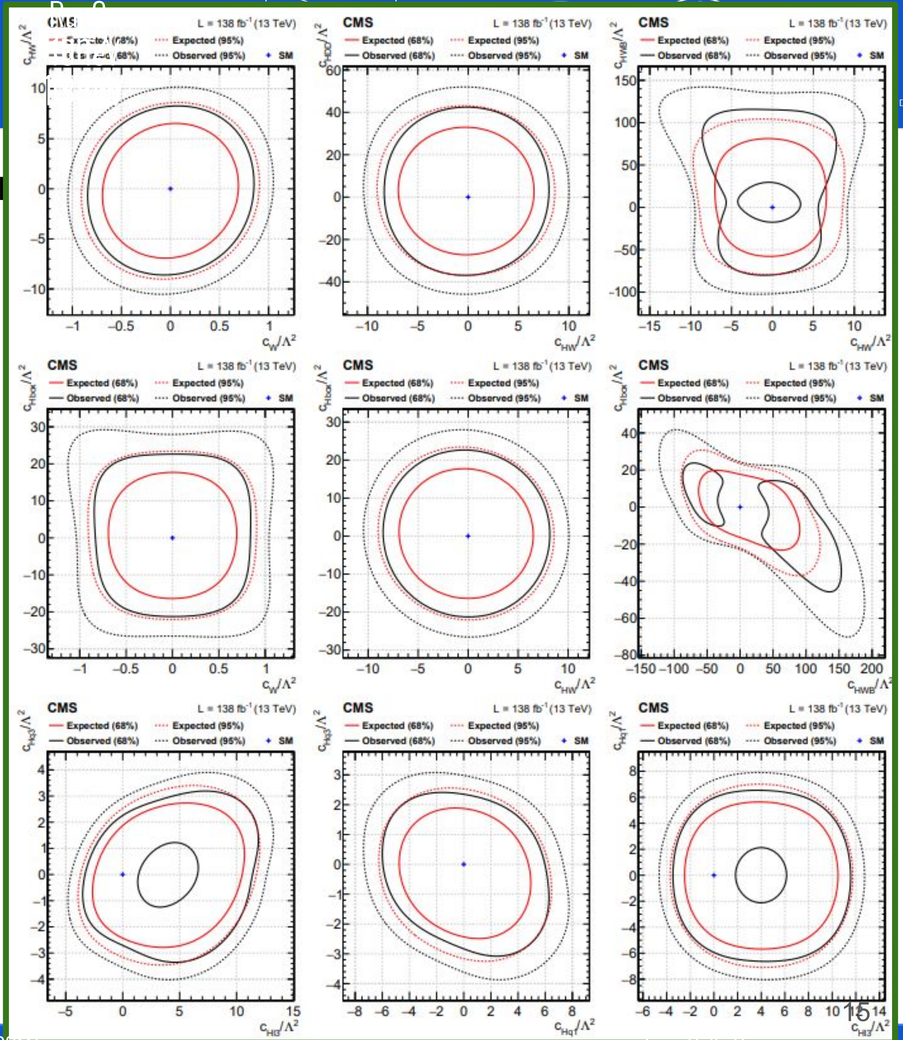

SMP-22-008
Submitted to JHEP

ssWW Vector Boson Scattering

Indirect search of BSM effects constraints dim-6 and dim-8 EFT operators
Extraction of dim-6 and dim-8 coefficients from scan likelihood fit

- one at a time (dim-6 or dim-8) putting to zero all the others
- 2D likelihood scan with 2 active dimension six operators
- 2D likelihood scan with one dim-6 + one dim-8 active operator

$$N_{\mathrm{exp}}^{i,\alpha} = N_{\mathrm{SM}} + \frac{c_i}{\Lambda^2} N_{\mathrm{Lin}}^{i} + \frac{c_i^2}{\Lambda^4} N_{\mathrm{Quad}}^{i} + \frac{f_\alpha}{\Lambda^4} N_{\mathrm{Lin}}^{\alpha} + \frac{f_\alpha^2}{\Lambda^8} N_{\mathrm{Quad}}^{\alpha}.$$

- first limits on dim-6 operators in VBS events
- first study with combined EFT operators with different dimensions

SMP-22-008
Submitted to JHEP

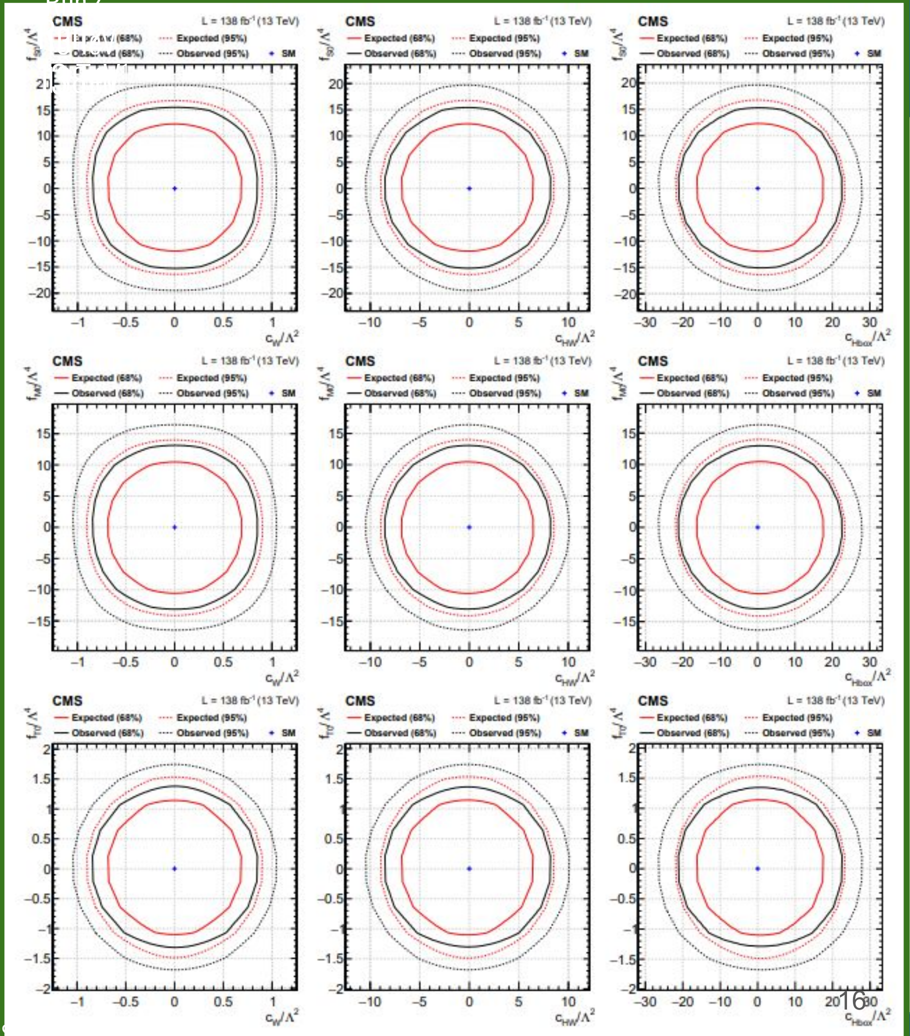

Observation of $\gamma\gamma \rightarrow \tau\tau$

Run2
13 TeV
138 fb^{-1}

Istituto Nazionale di Fisica Nucleare

$$pp \rightarrow \tau^+\tau^- p^* p^*$$

Leptons production via photon-photon fusion (pure QED process)
- clean topology when the protons remain intact (back-to-back lepton and no hadronic activity except for hadronically decay tau leptons)
- low N_{tracks} around the vertex and acoplanarity A cuts as proxy for back-to-back leptons, defining the SR

4 type of final states taken into account:

	$e\mu$	$e\tau_h$	$\mu\tau_h$	$\tau_h\tau_h$	$\mu\mu$
p_T^e (GeV)	> 15/24	> 25–33	—	—	—
$\lvert\eta^e\rvert$	< 2.5	< 2.1–2.5	—	—	—
p_T^μ (GeV)	> 24/15	—	> 21–29	—	> 26–29/10
$\lvert\eta^\mu\rvert$	< 2.4	—	< 2.1–2.4	—	< 2.4
$p_T^{\tau_h}$ (GeV)	—	> 30–35	> 30–32	> 40	—
$\lvert\eta^{\tau_h}\rvert$	—	< 2.1–2.3	< 2.1–2.3	< 2.1	—
$m_{\mu\mu}$ (GeV)	—	—	—	—	> 50
OS	yes	yes	yes	yes	yes
$\lvert d_z(\ell,\ell')\rvert$ (cm)	< 0.1	< 0.1	< 0.1	< 0.1	< 0.1
$\Delta R(\ell,\ell')$	> 0.5	> 0.5	> 0.5	> 0.5	> 0.5
$m_T(e/\mu p_T, \vec{p}_T^{miss})$ (GeV)	—	< 75	< 75	—	—

FIRST OBSERVATION
in pp collisions
5.3σ

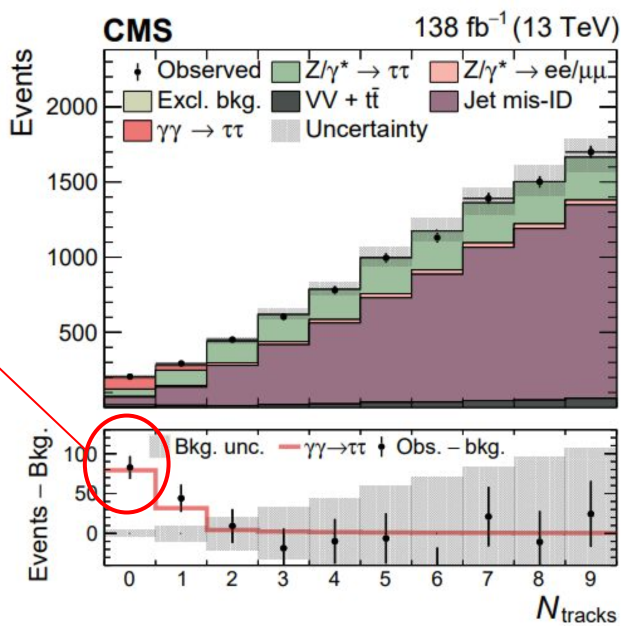

Rep. Prog. Phys. 87 (2024) 107801

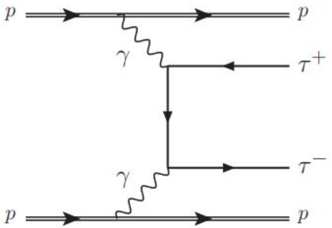

$$\Gamma^\mu = \gamma^\mu F_1(q^2) + \frac{\sigma^{\mu\nu} q_\nu}{2m}\left[iF_2(q^2) + F_3(q^2)\gamma_5\right]$$

Observation of $\gamma\gamma \to \tau\tau$

Run2
13 TeV
138 fb^{-1}

Leptons production via photon-photon fusion (pure QED process)

- clean topology when the protons remain intact (back-to-back lepton and no hadronic activity except for hadronically decay tau leptons)
- low N_{tracks} around the vertex and acoplanarity A cuts as proxy for back-to-back leptons, defining the SR

4 type of final states taken into account:

	$e\mu$	$e\tau_h$	$\mu\tau_h$	$\tau_h\tau_h$	$\mu\mu$
p_T^e (GeV)	$> 15/24$	> 25–33	—	—	—
$\lvert\eta^e\rvert$	< 2.5	< 2.1–2.5	—	—	—
p_T^μ (GeV)	$> 24/15$	—	> 21–29	—	> 26–$29/10$
$\lvert\eta^\mu\rvert$	< 2.4	—	< 2.1–2.4	—	< 2.4
$p_T^{\tau_h}$ (GeV)	—	> 30–35	> 30–32	> 40	—
$\lvert\eta^{\tau_h}\rvert$	—	< 2.1–2.3	< 2.1–2.3	< 2.1	—
$m_{\mu\mu}$ (GeV)	—	—	—	—	> 50
OS	yes	yes	yes	yes	yes
$\lvert d_z(\ell,\ell')\rvert$ (cm)	< 0.1	< 0.1	< 0.1	< 0.1	< 0.1
$\Delta R(\ell,\ell')$	> 0.5	> 0.5	> 0.5	> 0.5	> 0.5
$m_T(e/\mu p_T, \vec{p}_T^{miss})$ (GeV)	—	< 75	< 75	—	—

$$\sigma^{fid}_{obs} = 12.4^{+3.8}_{-3.1} \text{ fb}$$

in agreement with GAMMA-UPC generator

$$pp \to \tau^+\tau^- p^* p^*$$

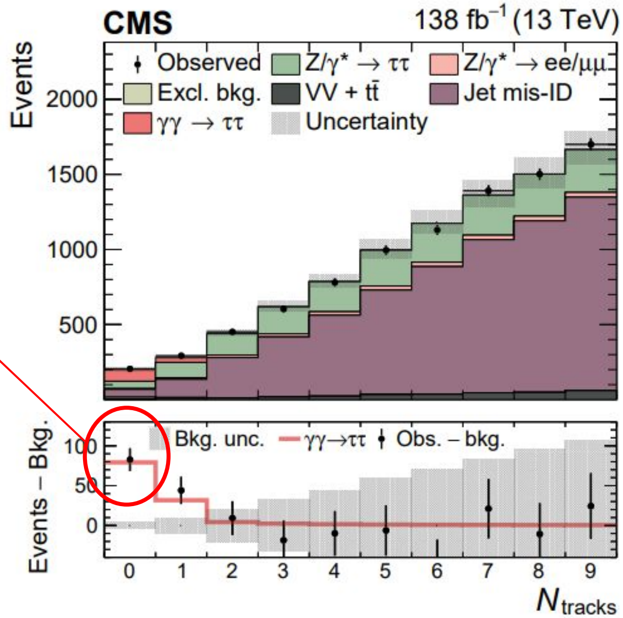

[Rep. Prog. Phys. 87 (2024) 107801]

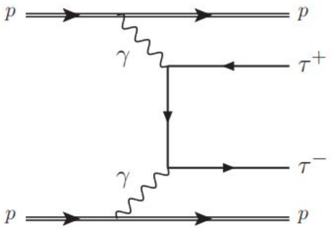

$$\Gamma^\mu = \gamma^\mu F_1(q^2) + \frac{\sigma^{\mu\nu} q_\nu}{2m}\left[iF_2(q^2) + F_3(q^2)\gamma_5\right]$$

Observation of $\gamma\gamma \to \tau\tau$

Run2
13 TeV
138 fb^{-1}

NOT ONLY OBSERVATION
BSM effects taken into account to account for the effect on the anomalous magnetic moment

- Larger values of a_τ results in more events for large values of m_{VIS} (blue line)

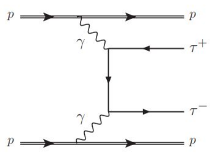

$$V_{\tau\tau\gamma} = ie\gamma^{\mu} - \frac{v\sqrt{2}}{\Lambda^2}\left[\mathrm{Re}\left[C_{\tau\gamma}\right] + \mathrm{Im}\left[C_{\tau\gamma}\right] i\gamma_5\right]\sigma^{\mu\nu}q_{\nu}$$

$$\delta d_\tau = \frac{\sqrt{2}v}{\Lambda^2}\mathrm{Im}\left[C_{\tau\gamma}\right]. \qquad \delta a_\tau = \frac{2m_\tau}{e}\frac{\sqrt{2}v}{\Lambda^2}\mathrm{Re}\left[C_{\tau\gamma}\right]$$

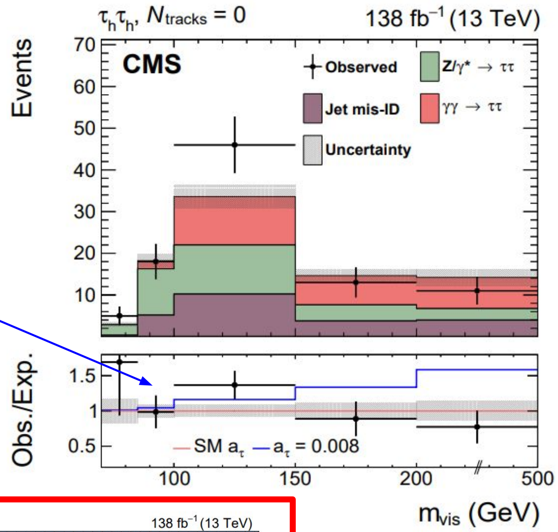

Binned maximum likelihood scan to extract a_τ and d_τ from m_{VIS} distributions

Constraints on Wilson coefficients

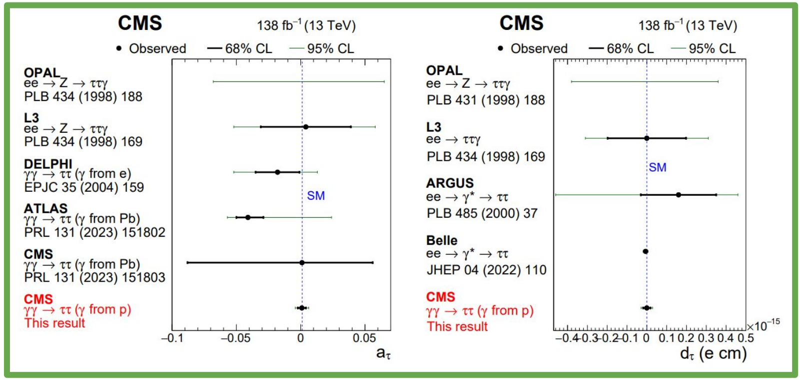

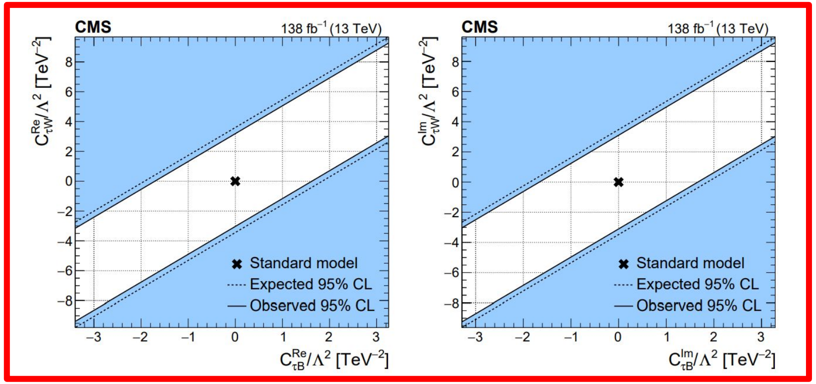

Rep. Prog. Phys. 87 (2024) 107801

Observation of $\gamma\gamma \rightarrow \tau\tau$

NOT ONLY OBSERVATION

BSM effects taken into account to account for the effect on the anomalous magnetic moment

- Larger values of a_τ results in more events for large values of m_{VIS} (blue line)

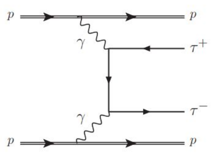

$$V_{\tau\tau\gamma} = ie\gamma^{\mu} - \frac{v\sqrt{2}}{\Lambda^2}\left[\mathrm{Re}\left[C_{\tau\gamma}\right] + \mathrm{Im}\left[C_{\tau\gamma}\right] i\gamma_5\right]\sigma^{\mu\nu}q_{\nu}$$

$$\delta d_\tau = \frac{\sqrt{2}v}{\Lambda^2}\mathrm{Im}\left[C_{\tau\gamma}\right]. \qquad \delta a_\tau = \frac{2m_\tau}{e}\frac{\sqrt{2}v}{\Lambda^2}\mathrm{Re}\left[C_{\tau\gamma}\right]$$

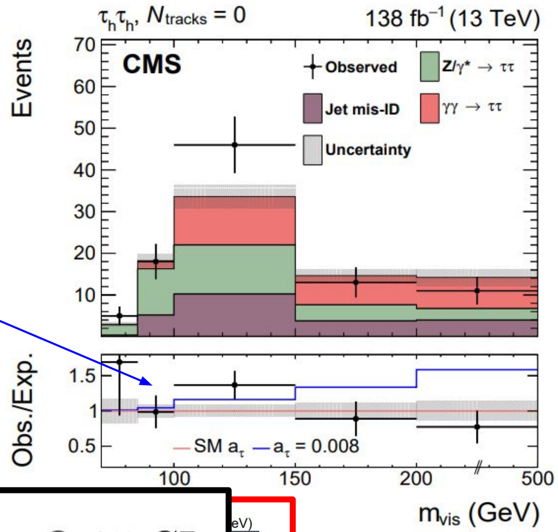

Binned maximum likelihood scan to extract a_τ and d_τ from m_{VIS} distributions

Constraints on Wilson coefficients

$$a_\tau = 0.0009^{+0.0032}_{-0.0031} \qquad |d_\tau| < 2.9 \times 10^{-17} e\ \mathrm{cm}\ @\ 95\ \mathrm{CL}$$

Both in agreement with SM prediction

Most stringent limit on magnetic moment of τ lepton

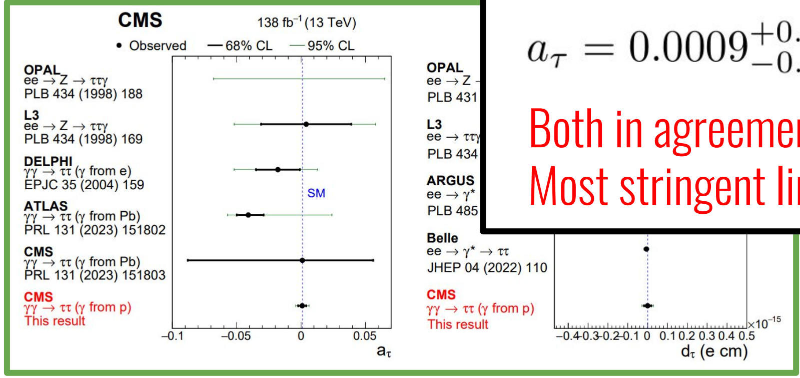

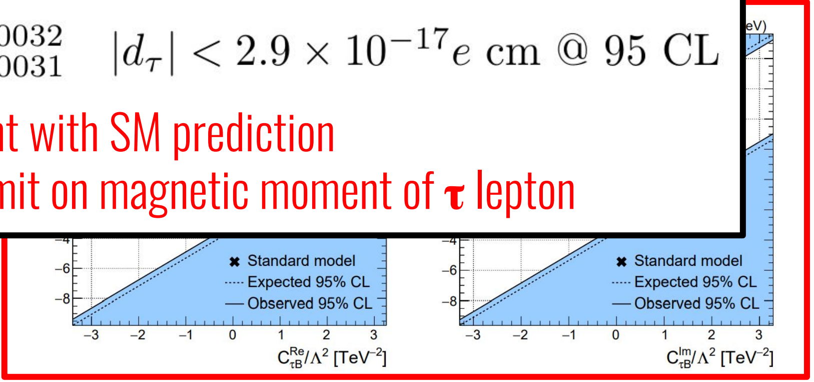

Rep. Prog. Phys. 87 (2024) 107801

Summary

CMS has different goals in the Electroweak Physics research

- Precision Measurement: recent results on SM parameters are comparable to, or exceed, the precision achieved at LEP
- Testing of the EW sector at high energy: multibosons final states are used to search for BSM effects and new observations

New results will be available soon from data collected at 13.6 TeV during Run-3

Not a complete review, many other analysis published or submitted during the last year (see the CMS SM Physics public results web page)

THANKS FOR YOUR ATTENTION!

XXXI Cracow EPIPHANY Conference
13-17 January 2025

BACKUP

PDFs and F-B asymmetry

Impact of the PDF on the forward-backward asymmetry:

PDFs affects the asymmetry due to two effects:

- up-type and down-type quarks have different neutral current couplings: we must know the contributions of each type of quark to the cross section
- $A_{FB}(|y|, m)$ is based on the rapidity definition of the dilepton system (direction of the negative lepton) that is Lorentz-boosted in the quark direction: diluted if the antiquark has a larger momentum w.r.t the quark

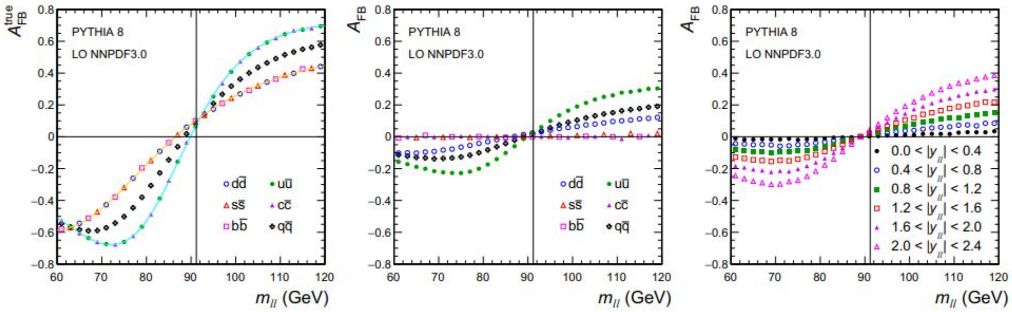

from the Run2 8 TeV analysis

definition of weighted $A_{FB}(|y|, m)$

$$\frac{1}{\sigma}\frac{d\sigma}{d\cos\theta^*} = \frac{3}{8}\left[1+\cos^2\theta^* + \frac{A_0}{2}(1-3\cos^2\theta^*) + A_4\cos\theta^*\right]. \quad (7)$$

The A_{FB} value in each $(m_{\ell\ell}, y_{\ell\ell})$ bin is calculated using the "angular event weighting" method, described in Ref. [40], in which each event with a $\cos\theta^*$ value (denoted as "c"), is reflected in the denominator (D) and numerator (N) weights through:

$$w_D = \frac{1}{2}\frac{c^2}{(1+c^2+h)^3}, \quad (8)$$

$$w_N = \frac{1}{2}\frac{|c|}{(1+c^2+h)^2}, \quad (9)$$

where $h = 0.5A_0(1-3c^2)$. Here, as a baseline we use the $p_{T,\ell\ell}$-averaged A_0 value of about 0.1 in each measurement $(m_{\ell\ell}, y_{\ell\ell})$ bin, as predicted by the signal MC simulation. Using the weighted sums N and D for forward ($\cos\theta^* > 0$) and backward ($\cos\theta^* < 0$) events, we obtain

$$D_F = \sum_{c>0} w_D, \quad D_B = \sum_{c<0} w_D, \quad (10)$$

$$N_F = \sum_{c>0} w_N, \quad N_B = \sum_{c<0} w_N, \quad (11)$$

from which the weighted A_{FB} of Eq. (2) can be written as:

$$A_{FB} = \frac{3}{8}\frac{N_F - N_B}{D_F + D_B}. \quad (12)$$

$A_4(|y|,m)$ unfolding

SMP-22-010
Submitted to Phys.Lett.B

We also extract $\sin^2\theta^{\ell}_{\text{eff}}$ through the unfolded A_4 measurements, at Born level, in the pre-FSR dilepton $|Y|$-M bins. The $A_4(|Y|, M)$ values are obtained by minimizing

$$\chi^2(\vec{p},\vec{v}) = |\vec{v}|^2 + \sum_i (D_i - T_i(\vec{p},\vec{v}))^T\, V_i^{-1}\,(D_i - T_i(\vec{p},\vec{v}))\,,$$

where i represents the four data-taking periods and four dilepton channels, $\vec{p}$ represents the parameters of interest, which are A_4 and the various weights (strength factors κ), $\vec{v}$ is the vector of all nuisance parameters, V is the covariance matrix, which includes the statistical uncertainties in data, signal MC simulations, backgrounds (MC simulation and CRs), efficiencies, calibration, and trigger prefiring probabilities, D is the observed numbers of data events in the $r = (|y|, m, \cos\theta_{\text{CS}})$ bins, and T is the vector of the corresponding predictions. For each sample and bin r,

$$T_r(\vec{p},\vec{v}) = \sum_g S_r^g(\vec{p},\vec{v}) + S_r^o(\vec{\kappa},\vec{v}) + B_r(\vec{v}),$$

where S_r^g is the signal contribution from the pre-FSR bin $g = (|Y|, M, C)$, with C being the pre-FSR $\cos\theta_{\text{CS}}$ bin, to the reconstructed bin r, calculated as

$$S_r^g(\kappa, A_4, A_0) = S_{r,0}^g\,\kappa\,\frac{\int_C f(x; A_4, A_0)\,\mathrm{d}x}{\int_C f(x; A_{4,0}, A_{0,0})\,\mathrm{d}x},$$

where $S_{r,0}^g$, $A_{4,0}$, and $A_{0,0}$ denote reference predictions evaluated from simulation, and

$$f(x; A_4, A_0) = 1 + x^2 + 0.5\,A_0\,(1 - 3x^2) + A_4\,x.$$

The S_r^o term represents the signal contribution from the underflow plus overflow pre-FSR bins to the reconstructed bin r. These predictions are scaled according to floating strength-factor values in the underflow and overflow measurement rapidity and mass bins. The B_r term represents the background contribution.

ssWW DNNs

Three discriminators: SM ssWW, dim-6 VBS and dim-8 VBS
A signature of VBS-like process is the large jets separation, features that are proxies of this topology are introduced in the DNNs

- Zeppenfeld variable: how much central are the leptons w.r.t VBS jets:

$$z_{\text{event}} = \frac{1}{2}\frac{\eta_\ell - \left|\frac{\eta_{j_1}+\eta_{j_2}}{2}\right|}{\eta_{j_1} - \eta_{j_2}} + \frac{1}{2}\frac{\eta_{\tau_h} - \left|\frac{\eta_{j_1}+\eta_{j_2}}{2}\right|}{\eta_{j_1} - \eta_{j_2}},$$

- Alignment of the leptons along the jet axis:

$$p_{\mathrm{T},1j}^{\mathrm{rel}} = \frac{|\vec{p}_1 \times \vec{p}_j|}{|\vec{p}_j|}.$$

DNN list of input features

Table 2: List of the input variables for the three DNN models developed in this study. The check mark indicates that the variable is included in the DNN model identified in the column header.

Input variable	SM DNN	dim-6 DNN	dim-8 DNN
τ_h p_T	✓	✓	✓
ℓ p_T	✓	✓	✓
τ_h η		✓	
ℓ η		✓	
leading VBS jet p_T	✓	✓	✓
subleading VBS jet p_T	✓	✓	✓
leading VBS jet mass		✓	✓
subleading VBS jet mass		✓	✓
VBS jet pair $\Delta\phi$		✓	
m_{jj}	✓	✓	
m_{1T}	✓	✓	✓
$m_{\circ 1}$	✓	✓	✓
$m_\mathrm{T}(\tau_\mathrm{h}, \vec{p}_\mathrm{T}^{\,\mathrm{miss}})$			✓
$m_\mathrm{T}(\ell, \vec{p}_\mathrm{T}^{\,\mathrm{miss}})$	✓	✓	✓
$m_\mathrm{T}(\ell + \tau_\mathrm{h}, \vec{p}_\mathrm{T}^{\,\mathrm{miss}})$			✓
$p_\mathrm{T}^\mathrm{rel}(\ell, j_1)$		✓	
$p_\mathrm{T}^\mathrm{rel}(\ell, j_2)$		✓	
$p_\mathrm{T}^\mathrm{rel}(\tau_\mathrm{h}, j_1)$		✓	
$p_\mathrm{T}^\mathrm{rel}(\tau_\mathrm{h}, j_2)$		✓	
$\Delta\phi(\ell, j_1)$		✓	
$\Delta\phi(\ell, j_2)$		✓	
$\Delta\phi(\tau_\mathrm{h}, j_1)$		✓	
$\Delta\phi(\tau_\mathrm{h}, j_2)$		✓	
$p_{\mathrm{T,\,leading}\ \tau_\mathrm{h}\ \mathrm{track}} / p_{\mathrm{T},\tau_\mathrm{h}}$	✓	✓	
z_{event}		✓	

Three discriminators: SM ssWW, dim-6 VBS and dim-8 VBS
A signature of VBS-like process is the large jets separation, features that are proxies of this topology are introduced in the DNNs.

- Energy distributions of WW pair:

$$m_{1T}^2 = \left(\sqrt{m_{\tau\ell}^2 + p_T^{\tau\ell\,2}} + p_T^{miss}\right)^2 - |\vec{p}_T^{\,\tau\ell} + \vec{p}_T^{\,miss}|^2,$$

$$m_{\circ 1}^2 = \left(p_T^{\tau} + p_T^{\ell} + p_T^{miss}\right)^2 - |\vec{p}_T^{\,\tau} + \vec{p}_T^{\,\ell} + \vec{p}_T^{\,miss}|^2.$$

DNN list of input features

Table 2: List of the input variables for the three DNN models developed in this study. The check mark indicates that the variable is included in the DNN model identified in the column header.

Input variable	SM DNN	dim-6 DNN	dim-8 DNN
$\tau_h\ p_T$	✓	✓	✓
$\ell\ p_T$	✓	✓	✓
$\tau_h\ \eta$		✓	
$\ell\ \eta$		✓	
leading VBS jet p_T	✓	✓	✓
subleading VBS jet p_T	✓	✓	✓
leading VBS jet mass		✓	✓
subleading VBS jet mass		✓	✓
VBS jet pair $\Delta\phi$		✓	
m_{jj}	✓	✓	
m_{1T}	✓	✓	✓
$m_{\circ 1}$	✓	✓	✓
$m_T(\tau_h, \vec{p}_T^{\,miss})$			✓
$m_T(\ell, \vec{p}_T^{\,miss})$	✓	✓	✓
$m_T(\ell + \tau_h, \vec{p}_T^{\,miss})$			✓
$p_T^{rel}(\ell, j_1)$		✓	
$p_T^{rel}(\ell, j_2)$		✓	
$p_T^{rel}(\tau_h, j_1)$		✓	
$p_T^{rel}(\tau_h, j_2)$		✓	
$\Delta\phi(\ell, j_1)$		✓	
$\Delta\phi(\ell, j_2)$		✓	
$\Delta\phi(\tau_h, j_1)$		✓	
$\Delta\phi(\tau_h, j_2)$		✓	
$p_{T,\text{leading } \tau_h \text{ track}} / p_{T,\tau_h}$	✓	✓	
z_{event}		✓	

$\gamma\gamma \rightarrow \tau\tau$: tracks multiplicity

Treatment of tracks multiplicity coming from PU or UE/hard scattering: we're looking at low tracks for SR (0 or 1 tracks)
Using muons to extract informations:

- PU correction: check the DY data and MC far from the muon dilepton vertex from the Z decay:

$$z^{\mathrm{corr}} = z_{\mathrm{BS}}^{\mathrm{corr}} + \frac{\sigma_{\mathrm{BS}}^{\mathrm{corr}}}{\sigma_{\mathrm{BS}}^{\mathrm{sim}}} \left(z - z_{\mathrm{BS}}^{\mathrm{sim}}\right).$$

- Hard Scattering: compare DY data/MC near the muon dilepton vertex and extract corrections for values of acoplanarity A in the regions A<0.015 and A>0.015, separately

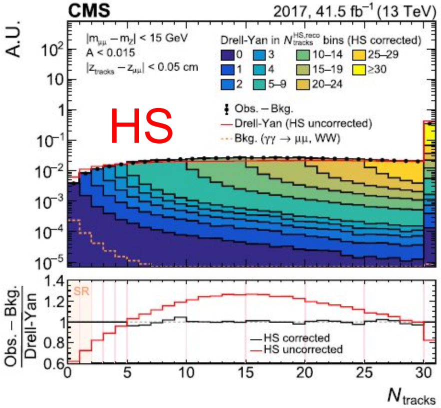

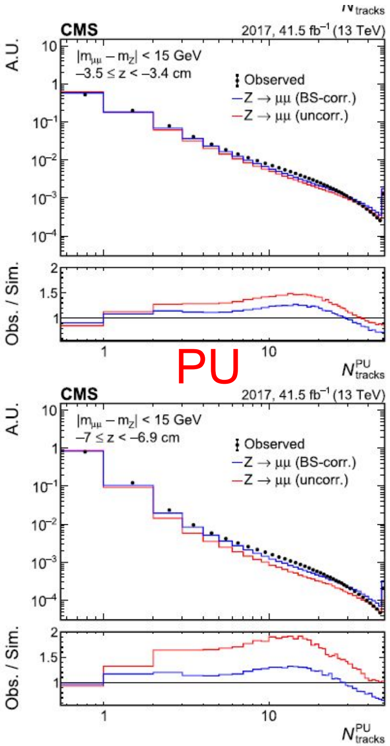

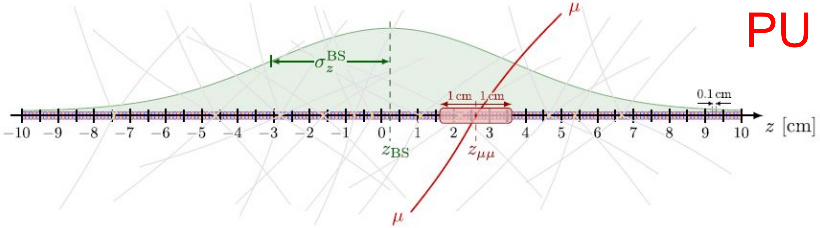

SMP-24-007	Determination of the strong coupling and its running from measurements of inclusive jet production	Submitted to PLB	21 December 2024
SMP-24-009	Measurement of the W boson decay branching fraction ratio $\mathcal{B}(W \to cq)/\mathcal{B}(W \to qq')$ in proton-proton collisions at $\sqrt{s} = 13$ TeV	Submitted to PLB	20 December 2024
SMP-23-002	High-precision measurement of the W boson mass with the CMS experiment at the LHC	Submitted to Nature	18 December 2024
SMP-24-005	Measurement of the inclusive WZ production cross section in pp collisions at $\sqrt{s} = 13.6$ TeV	Submitted to JHEP	3 December 2024
SMP-23-006	Proton reconstruction with the TOTEM Roman pot detectors for high-β^* LHC data	Submitted to JINST	29 November 2024
SMP-22-012	Search for rare decays of the Z and Higgs bosons to a J/ψ or $\psi(2S)$ meson and a photon in proton-proton collisions at $\sqrt{s} = 13$ TeV	Submitted to PLB	22 November 2024
SMP-22-008	Study of same-sign W boson scattering and anomalous couplings in events with one tau lepton from pp collisions at $\sqrt{s} = 13$ TeV	Submitted to JHEP	5 October 2024
SMP-22-010	Measurement of the Drell-Yan forward-backward asymmetry and of the effective leptonic weak mixing angle in proton-proton collisions at $\sqrt{s} = 13$ TeV	Submitted to PLB	14 August 2024
SMP-20-004	Measurement of the inclusive cross sections for W and Z boson production in proton-proton collisions at $\sqrt{s} = 5.02$ and 13 TeV	Submitted to JHEP	7 August 2024
SMP-24-001	Measurement of inclusive and differential cross sections for W^+W^- production in proton-proton collisions at $\sqrt{s} = 13.6$ TeV	Accepted by PLB	7 June 2024
SMP-23-005	Observation of $\gamma\gamma \to \tau\tau$ in proton-proton collisions and limits on the anomalous electromagnetic moments of the τ lepton	ROPP 87 (2024) 107801	2024-09-02
SMP-23-004	Stairway to discovery: a report on the CMS programme of cross section measurements from millibarns to femtobarns	Accepted by PR	29 May 2024
SMP-22-016	Search for the Z boson decay to $\tau\tau\mu\mu$ in proton-proton collisions at $\sqrt{s} = 13$ TeV	PRL 133 (2024) 161805	2024-10-18
SMP-22-005	Measurement of multijet azimuthal correlations and determination of the strong coupling in proton-proton collisions at $\sqrt{s} = 13$ TeV	EPJC 84 (2024) 842	2024-08-21
SMP-22-001	Measurement of differential ZZ+jets production cross sections in pp collisions at $\sqrt{s} = 13$ TeV	JHEP 10 (2024) 209	2024-10-29
SMP-22-015	Measurement of energy correlators inside jets and determination of the strong coupling $\alpha_S(m_Z)$	PRL 133 (2024) 071903	2024-08-14
SMP-21-004	Nonresonant central exclusive production of charged-hadron pairs in proton-proton collisions at $\sqrt{s} = 13$ TeV	PRD 109 (2024) 112013	2024-06-11